frontiers | Frontiers in Ecology and Evolution

TYPE Original Research
PUBLISHED 23 August 2023
DOI 10.3389/fevo.2023.1264936

OPEN ACCESS

EDITED BY
Haijun Qiu,
Northwest University, China

REVIEWED BY
Kang Liao,
China University of Geosciences Wuhan, China
Zongxing Zou,
China University of Geosciences Wuhan, China

*CORRESPONDENCE
Zhenwei Dai
daizhenwei@mail.cgs.gov.cn

RECEIVED 21 July 2023
ACCEPTED 04 August 2023
PUBLISHED 23 August 2023

CITATION
Zhang A, Dai Z, Qin W, Fu X, Gao J, Guo L, Liu L, Jiang X and Wang H (2023) Risk assessment of the Xigou debris flow in the Three Gorges Reservoir Area. *Front. Ecol. Evol.* 11:1264936. doi: 10.3389/fevo.2023.1264936

Risk assessment of the Xigou debris flow in the Three Gorges Reservoir Area

Anle Zhang[1,2], Zhenwei Dai[1]*, Weibing Qin[3], Xiaolin Fu[1], Jingxuan Gao[4,5], Lianjun Guo[6], Liang Liu[6,7], Xiannian Jiang[8] and Heng Wang[8]

[1]Wuhan Center, China Geological Survey (Geosciences Innovation Center of Central South China), Wuhan, Hubei, China, [2]College of Civil Engineering & Architecture, China Three Gorges University, Yichang, Hubei, China, [3]River Basin Hub Operation Management Center, China Three Gorges Corporation, Yichang, Hubei, China, [4]College of Geological Engineering and Geomatics, Chang'an University, Xi'an, China, [5]China Institute of Geological Environment Monitoring, Beijing, China, [6]The Eighth Geological Brigade, Hebei Bureau of Geology and Mineral Resources Exploration, Qinhuangdao, China, [7]School of Earth Sciences and Engineering, Nanjing university, Nanjing, China, [8]No. 208 Hydrogeology and Engineering Geology Team of Chongqing Bureau of Geology and Minerals Exploration, Chongqing, China

On June 18, 2018, under the influence of heavy rainfall, a debris flow disaster broke out in Xigou village of the Three Gorges Reservoir Area in Chongqing, causing some residential houses to be buried along with great economic losses. The on-site investigation found many loose solid material sources in the debris flow gully. Under the conditions of heavy rainfall, debris flows are prone to occur again, which would seriously threaten the lives and property of nearby residents. In this paper, taking the Xigou debris flow as a research case, numerical simulation by rapid mass movements simulation (RAMMS) is used to invert the movement process of the 2018 debris flow event; the dynamic calculation parameters of the Xigou debris flow event are obtained; a quantitative hazard prediction of debris flows with different recurrence intervals (30, 50, and 100 years) is carried out in the study area; and risk assessment is conducted based on the vulnerability characteristics of the disaster-bearing bodies in the study area. The results show that the maximum accumulation thickness of debris flow in the 30-year, 50-year, and 100-year recurrence intervals is 6.54 m, 10.18 m, and 10.00 m, respectively, and the debris flow in the 100-year recurrence interval has the widest influence range and greatest hazard. The low-, medium-, and high-risk areas account for 75%, 23%, and 2%, respectively. The high-risk area mainly includes some buildings near the #1 and #2 gullies. This study provides support for the prevention and control of potential debris flow disasters in Xigou village and a scientific basis for disaster prevention and mitigation in the Three Gorges Reservoir area.

KEYWORDS

Three Gorges Reservoir Area, debris flow, RAMMS, analysis of movement characteristics, risk assessment

1 Introduction

Debris flow is a common geological disaster in the mountainous areas of Southwest China. Characterized by high speed, suddenness, and high energy, it often causes serious economic losses and casualties (Yu et al., 2010; Tang et al., 2012; Zou et al., 2020; Qin et al., 2022; Dai et al., 2023a; Dai et al., 2023b). The Three Gorges Reservoir area has large undulating topography, complex strata and lithology, intense geological tectonic activities, frequent extreme rainfall events, and intense human activities (engineering constructions) (Yin et al., 2020; Zou et al., 2023), which have created favorable conditions for debris flows in the area. The population of the Three Gorges Reservoir area has grown more concentrated after the area's resettlement project. After a debris flow occurs in a resettlement area, it could cause huge losses of life and property (Wang et al., 2018; Zhang et al., 2019; Guo et al., 2020; Zhang et al., 2021; Qiu et al., 2022; Zhang et al., 2022; Dai et al., 2023c; Pei et al., 2023). Many mountain towns in China are located on the joint alluvial fans of multiple and adjacent past debris flows (Cui et al., 2013). During heavy rainfall, multiple debris flows can easily break out at the same time, leading to disasters of various forms. In addition to direct dynamic impact destruction, debris accumulation, and subsequent damage induced by lifeline destruction and chain-reaction disasters that occur due to river blockages. Therefore, it is urgent to clarify the movement process of debris flows and evaluate the hazard and risk areas for the prevention of debris flow disasters in the Three Gorges Reservoir area.

Debris flow disaster risk refers to the likelihood of loss of human life, property, economic activities, etc., due to a debris flow disasters within a certain area within a certain time (Liu et al., 2012). The core of risk assessment is hazard and vulnerability assessments of debris flows. As computer technology and numerical calculation methods have advanced, numerical calculations can not only reflect the velocity variation characteristics of debris flows but also yield intuitive information such as the influence range of debris flows, and are an effective method for the quantitative debris flow hazard assessment.

In recent years, scholars have performed much research on the hazards and risk assessment of debris flows (Ouyang et al., 2019; Lai et al., 2021; Wang et al., 2022; Dai et al., 2023c), and proposed various methods and models to carry out risk assessments of single-gully debris flows. Zhang et al. (2014) applied FLO-2D to simulate three debris-flow gullies in Qingshuigou, Zuizizigou, and Duanheba, and achieved good results. Gentile et al. (2008) assessed the hazard degrees of four types of debris flow by analyzing the hazards of debris flows in southern Italy. Calvo and Savi (2009) proposed a method for risk analysis of debris flow-prone areas, applied Monte Carlo procedures to debris flows in Valtellina in the Alps, and explored the impact of different vulnerability functions on risk.

Many scholars have carried out debris flow simulations and achieved valuable results, but most of the research has focused on the risk assessment of a single-gully debris flow and have rarely considered the harm caused by the simultaneous eruption of multiple debris flows. Although the method of hazard and vulnerability has been widely used in the risk assessment of single natural disasters, there are still many challenges for the risk assessment of complex disasters.

In this paper, taking the Xigou debris flows in the Three Gorges Reservoir area as a research case, numerical simulation by RAMMS is used for the inversion of the movement process of the 2018 debris flow event. The dynamic calculation parameters of the debris flow in Xigou are obtained; a quantitative hazard prediction of debris flows with different recurrence intervals (30, 50, and 100 years) in the study area when debris flows simultaneously break out in multiple gullies is carried out; and risk assessment is conducted based on the vulnerability characteristics of the disaster-bearing body in the study area. This study can provide empirical and theoretical support for the prevention and control of debris flow disasters in Xigou village and can serve as a reference for the prevention and control of debris flow disasters in the Three Gorges Reservoir area.

2 Geological background of the study area

The Xigou debris flow is located in Wushan County, Chongqing (31°09′16″ N, 109°58′34″ E). The terrain of the study area is high in the north and low in the south, with an altitude of 265-1890 m. The terrain is steep at the top and gentle at the bottom. The upper part of the valley has steep slopes (30° to 50°), and the lower part has gentle slopes (10° to 20°). There are three debris-flow gullies in this area. The basins of the #1, #2, and #3 debris-flow gullies are all rectangular in shape. The valley trend is 10° southeast, the cross-section has a V shape, the channel is straight, and the overall basin area is approximately 0.479 km² (Figure 1). The topographic information of the debris flow basin is shown in Table 1.

The study area is located in the southeast flank of the Qiyaoshan anticline, with a monoclinic output. The strata occurrence is 160-180°∠45-58°. No faults are developed. The strata distributed in this area are the Quaternary artificial filling soil (Q_4^{ml}), Quaternary Holocene landslide accumulation layer (Q_4^{del}), Quaternary colluvial soil layer (Q_4^{col+dl}), and Quaternary Pleistocene alluvial-diluvial layer (Q_4^{al+pl}). The exposed bedrock is mainly Triassic Badong Formation (T_2b) mudstone, fractured marl, and Lower Triassic Jialingjiang Formation (T_1j^4) limestone. Some weak interlayers and loose accumulation layers are distributed in each channel, providing good material source conditions for the formation of debris flows.

The study area has a subtropical monsoon humid climate, with an annual average temperature of 18.4 °C, an annual average rainfall of 1066.22 mm, a maximum annual rainfall of 1509.9 mm, a maximum monthly rainfall of 445.9 mm (September), and a maximum daily rainfall of 384.6 mm (August 31, 2014), and 68.8% of the rainfall occurs in the rainy season (May-September). From January to August in 2018, the cumulative rainfall was 824.8 mm, and the cumulative rainfall in June reached 194.2 mm, far exceeding the historical average rainfall of June (Figure 2), which provided external triggering conditions for the debris flow.

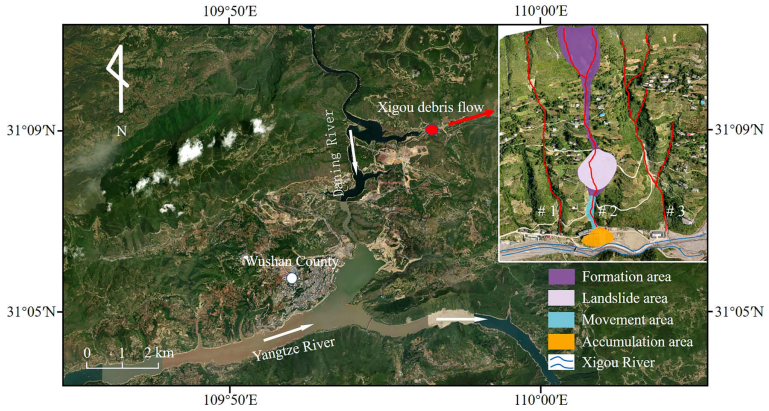

FIGURE 1
Geographic location and movement zones of the Xigou debris flow.

On June 18, 2018, Wushan County suffered continuous heavy rainfall adding up to 174.3 mm. Due to the rainfall, many small landslides occurred on the rear edge of the slope and accumulated in the ditch to mix with the rainwater in the ditch, resulting in debris flow disasters. According to the movement characteristics of the debris flow in gully #2, there are three areas: formation area, movement area, and accumulation area. There is a landslide area in the formation area (Figure 1).

In the formation area, the elevation is mainly 310-560 m, the slope is approximately 30°, and the overall area is approximately 0.448 km^2. The overburden layer on the slope surface is mainly gravel soil of avalanche deposits, the thickness of the soil layer is approximately 20 m, and the strongly weathered bedrock is exposed locally. The phenomenon of collapses and shallow landslides in this area is relatively serious, providing much loose solid for debris flows.

The movement area stretches 135 m long, mainly located between the elevation of 310 m and the debris flow channel outlet. The channel is generally narrow and straight, which is conducive to the rapid flow of debris. Many deposits can be seen along the valley in this area, resulting in a significant narrowing of the channel and obvious signs of erosion on the sidewall and bottom of the channel.

The accumulation area is located near the debris flow channel outlet. With flat terrain and an open space, it is shaped like a fan and spans approximately 6,643 m^2. This area is where residential houses and infrastructure are concentrated.

Geographically, gullies #1, #2, and #3 are located from west to east. Since the three debris-flow gullies are adjacent and are located

TABLE 1 Topographic information of #1, #2, and #3 debris-flow gullies.

Name	Basin area (km^2)	Length (km)	Elevation difference (m)	Average slope (°)	Vegetation cover (%)
#1	0.111	0.76	260	27	75
#2	0.159	0.81	280	29	70
#3	0.209	0.87	255	26	80

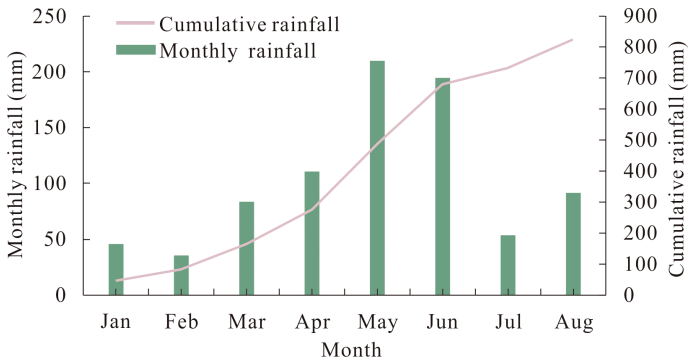

FIGURE 2
Monthly and cumulative rainfall in the study area in 2018. Modified according to reference Dai et al., 2023c.

on the same slope, their valley characteristics and topography are relatively similar. In short, the debris flow channel is narrow and straight, the elevation difference is nearly 300 m, the slope is steep, and the rock mass is severely weathered. There are serious collapses and shallow landslides in the upper reaches of the gully, and much loose soil remains in the gully, which provides a rich solid material source for the formation of debris flows. Seasonal rainfall varies widely in this area, with abundant rainfall in summer, accounting for approximately 65% of the annual rainfall, when the area is prone to landslides, debris flows, and other disasters. The topography, provenance, water source, and other conditions of the study area are conducive to the formation of debris flows. Therefore, the study area has the conditions for the eruption of debris flows. Affected by extreme rainfall and human activities (engineering constructions) in recent years, slope erosion and soil erosion have intensified, and the amount of loose solid material sources has increased greatly, resulting in a possible decrease in the critical rainfall intensity that will trigger debris flows and an increase in the frequency of debris flows.

At present, some villagers in Xigou village live on slopes and at the debris flow channel outlet. Once debris flows erupt, many people's lives and property can be lost. Therefore, it is very important to carry out disaster risk assessments of debris flows in Xigou village.

3 Numerical simulation and inversion of the Xigou debris flow

On June 18, 2018, a debris flow disaster occurred in gully #2 in the study area. In this section, we reproduce the 2018 debris flow event by numerical simulation, and reasonable calculation parameters and calculation models are obtained by inversion. Finally, the validated parameters and model are used to predict the scope of the influence of debris flows with different recurrence intervals and risk assessments.

3.1 Introduction to RAMMS

The RAMMS software was developed by the Swiss Federal Institute for Snow and Avalanche Research. It is mainly used to simulate the whole process of avalanches, collapses, debris flows, and shallow landslides from initial failure to movement and accumulation on 3D terrain. The DEBRIS-FLOW module (that is, the debris flow module) in the software can predict the spatial distribution of data, such as debris flow movement paths, flow velocities, flow depths, and pressure, allowing for better numerical simulation of the movement of debris flows (Christen et al., 2010).

In the RAMMS model, debris flow is regarded as a fluid with rheological properties. The Voellmy–Salm rheological continuum model is used to address rheological problems, the laws of material energy and motion transformation are used to address the movement and accumulation process of debris flow, and the random kinetic energy (RKE) model is used to make additional adjustments. In this study, the dynamic characteristics of the parameters are analyzed to obtain the desired simulation results.

3.1.1 Voellmy–Salm rheological model

The movement characteristics of debris flows are determined by two main parameters: the debris flow depth H (x, y, t) and the flow velocity U (x, y, t). The flow depth is expressed as follows:

$$\partial_t H + \partial_x (HU_x) + \partial_y (HU_y) = Q(x, y, t) \tag{1}$$

where H represents the fluid height (m) and $Q(x, y, t)$ is the mass source [kg/(m^2·s)]; $Q = 0$ means no material deposition.

The flow velocity is expressed as follows:

$$\| U \| = \sqrt{U_x^2 + U_y^2} \tag{2}$$

where $\| U \|$ means the absolute average velocity U, so as to make sure that U is a strictly positive velocity in the vector space. The direction of fluid velocity is:

$$n_U = \frac{1}{\| U \| (U_x, U_y)} \tag{3}$$

The frictional resistance of the Voellmy–Salm rheological model is determined by the following Equations:

$$S_f = (S_{fx} + S_{fy}) \tag{4}$$

$$S_{fx} = nU_x[\mu g_z H + \frac{g \| U \|^2}{\xi}] \tag{5}$$

$$S_{fx} = nU_y[\frac{\mu g_z H + g \| U \|^2}{\xi}] \tag{6}$$

In each Equation, x, y, and z are the coordinates in the Cartesian coordinate system, with x, y being the surface coordinates and z being the elevation; U is the average velocity of the debris flow; S_f is the frictional resistance; μ is the Coulomb friction coefficient; ξ is the turbulent flow friction coefficient; t is the movement time of the debris flow; and g is the acceleration due to gravity.

3.1.2 RKE model

The RKE model can make real-time adjustments to correct the debris flow simulation process. Due to the chaotic change in the fluid velocity and direction, the RKE model divides the flow velocity U into the average velocity and the instantaneous velocity. The flow velocity in the x and y directions is the vector sum of the average velocity and instantaneous velocity, and the average velocity in the z direction is set to 0 to better represent the real-time movement characteristics of the debris flow (Christen et al., 2010). In the RKE model, the friction coefficient μ and turbulence coefficient ξ play important roles.

The friction coefficient μ equals:

$$\mu(R) = \mu_0 exp(-\frac{R}{R_0}) \tag{7}$$

The turbulence coefficient ξ equals:

$$\xi(R) = \xi_0 exp(\frac{R}{R_0}) \quad (8)$$

where μ_0 is the static dry Coulomb, ξ_0 is the turbulence friction coefficients, R_0 is a constant (defined as the exponential growth rate of friction representing a random kinetic energy density function), and R is the depth-averaged random kinetic energy.

3.2 Numerical simulation of debris-flow gully #2

Based on unmanned aerial vehicle (UAV) aerial imagery data, a digital elevation model (DEM) with a resolution of 0.98 m was established. After importing the digital elevation model into RAMMS software, the grid size was set to 2 m, and the basin range and material source area were delineated. According to the actual situation, a value is assigned to the material source thickness, the simulation parameters are adjusted, and the three-point method is used to generate a flow curve (detailed parameters in Table 2).

According to the on-site investigation, debris flowed out from the side of the residential building and accumulated in a fan shape at the debris flow channel outlet (Figures 3A, B). Figure 3B shows the damage to the residential building when the debris flows occurred in 2018. The residential building was hit by the debris flows from the front. Doors, windows, and walls were severely damaged, and one wall was partially damaged. The first floor was buried. The debris flows accumulated behind the residential building with a thickness up to 2 stories high.

The thickness of the simulated debris flow in Figure 3C is 5.74 m, and the simulated debris flow is located near the northeast corner of the residential building, which is basically consistent with the actual accumulation range and thickness of the 2018 debris flow. Therefore, the 2018 debris flow event as reproduced using the current calculation model and parameters has good accuracy and reliability.

For the 2018 debris flow event, the debris flow depths at t=0 s, 80 s, 160 s, 240 s, 320 s, and 400 s are shown in Figure 4. Initially, the debris flow does not move, and the depth of the debris flow at t=0 represents the thickness of the unstable material source in the gully. In the landslide area at the end of the formation area, the phenomena of collapse and shallow landslides are more serious, and there are many loose solid material sources, so the material source in the landslide area is relatively thick. At t=80 s, the head of the debris flow passes through the movement area to the channel outlet, and the debris flow entrains many loose solids in the landslide area to flow downstream and accumulate in the narrow movement area. At t=160 s, the head of the debris flow rushes out of the channel outlet and hits nearby residential buildings, damaging some residential buildings. At t=240 s, with the continuous movement of the debris flow, the head of the debris flow, after

TABLE 2 Inversion parameters of the 2018 debris flow event.

Density ρ (g/cm^3)	Gravity g (m/s^2)	Average slope ψ (°)	Friction coefficient μ	Turbulence coefficient ξ
1.61	9.8	29	0.25	300

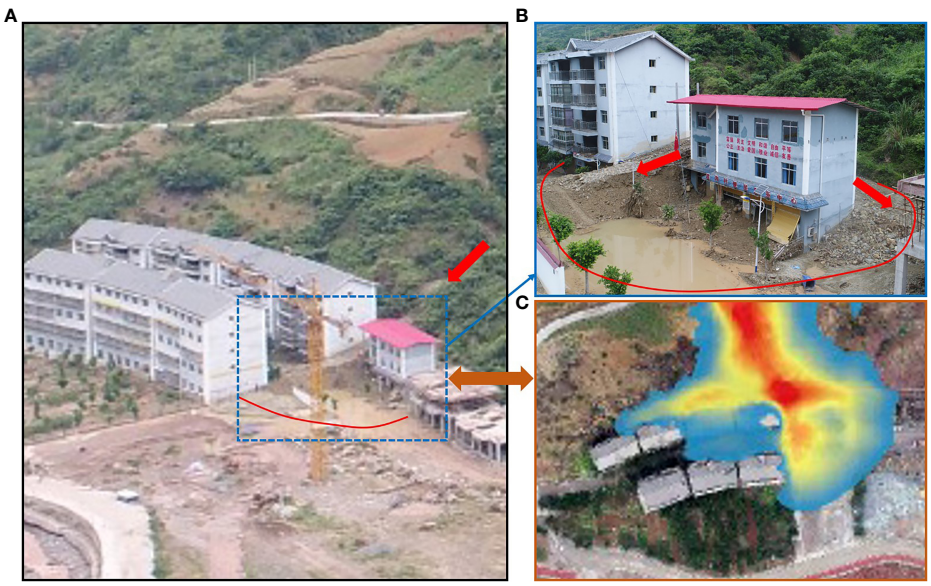

FIGURE 3
Photographs of the 2018 Xigou debris flow event. **(A)** Actual accumulation pattern. **(B)** Damage to residential buildings. **(C)** Simulated accumulation pattern.

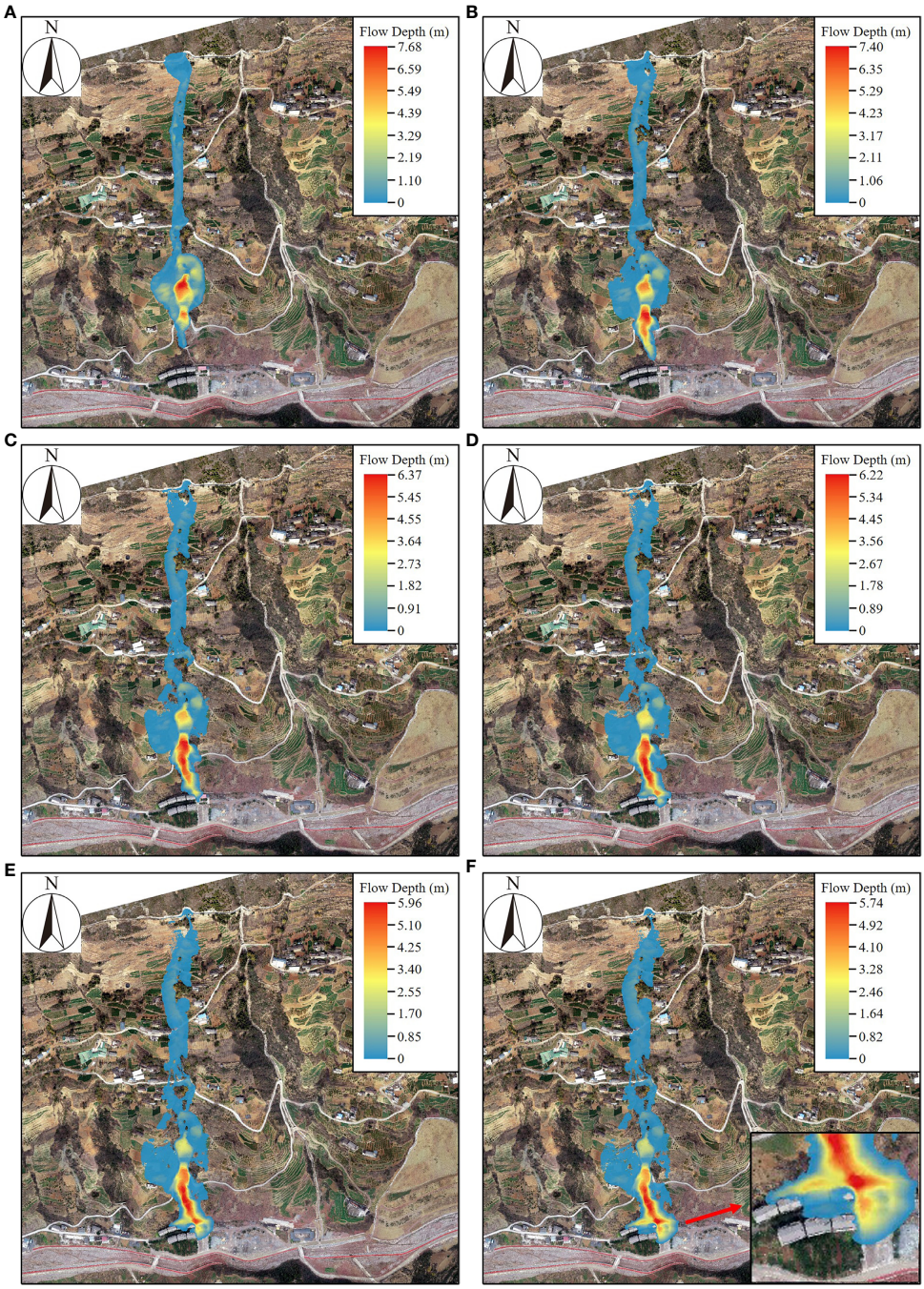

FIGURE 4
State of the Xigou debris flow at different times. **(A)** t=0 s, **(B)** t=80 s, **(C)** t=160 s, **(D)** t=240 s, **(E)** t=320 s, **(F)** t=400 s.

being blocked by the residential building, flows in two directions on the rear and the east side of the residential building. At t=320 s, the debris flow reaches the flat area and gradually accumulates in the rear and east of the residential building. At t=400 s, the debris flow stops moving. At this time, the debris flow depth is the accumulation thickness, and the debris flow forms a fan-shaped accumulation area at the channel outlet. The maximum accumulation thickness is 5.74 m, which happens near the northeast corner of the residential building.

4 Prediction and analysis of debris flow in the study area

In this paper, the rain-flood method is used to calculate the peak flow of debris flow. If debris flow and heavy rain occur at the same frequency and synchronously, the peak storm water flow in the sub-basin at different frequencies of the section is first calculated according to the hydrological method, and then the blockage

factor is chosen to calculate the debris flow according to the following Equation:

$$Q_c = (1 + \varnothing)Q_p D_c \quad (9)$$

where Q_c is the peak flow of debris flow with frequency P (m^3/s); $\varnothing$ is the sediment correction coefficient of debris flow; Q_p is the design flow for a rainstorm flood with frequency P (m^3/s); and D_c is the debris flow blockage coefficient.

$$\varnothing = (\gamma_c - \gamma_w)/(\gamma_H - \gamma_c) \quad (10)$$

where γ_c is the bulk density of the debris flow (kg/m^3); γ_w is the bulk density of clean water (kg/m^3), with γ_w =1.0 kg/m^3; and γ_H is the bulk density of solid matter in the debris flow (kg/m^3), with γ_H =2.65 kg/m^3.

Flood peak flow can be calculated by empirical formulas widely used by urban construction and water conservancy departments in the study area:

$$Q_p(1\,\%) = 11.2F^{0.84} \quad (11)$$

where $Q_p(1\,\%)$ is the design flow for storm floods with a 100-year recurrence interval (m^3/s), and F is the basin area (km^2). For the Three Gorges Reservoir area, the peak flood flow with different frequencies has the following empirical distribution: $Q_p(2\,\%)$ =0.8 $Q_p(1\,\%)$, $Q_p(3.3\,\%)$ =0.6 $Q_p(1\,\%)$, of which $Q_p(2\,\%)$, $Q_p(3.3\,\%)$ indicates the design flow (m^3/s) of the storm flood with a 50-year recurrence interval and a 30-year recurrence interval, respectively.

The calculation results are shown in Table 3.

The key to numerical simulation of debris flow is the determination of μ and ξ. Based on the inversion of the 2018 debris flow event, the specific μ and ξ are obtained. Corresponding models and related parameters are used to analyze and predict the potential impact range of debris flows in different return periods.

Figures 5A–C shows the accumulation thickness and influence range of the debris flow at different return periods. The common feature of the three return periods is that the debris flow hazards occur at gullies #1, #2, and #3 simultaneously, the differences being mainly the accumulation thickness of debris flow and the scope of the hazard area. For the debris flow with a 30-year recurrence interval, the maximum accumulation thickness in gully #1 is 4 m, and its head touches the houses and other buildings at the channel outlet, which poses a certain threat to the residents at the channel outlet. After the debris flow occurred in ditch #2 in 2018, some debris flow material sources remained in the gully. Therefore, under this condition, the potential hazard area of debris flow in gully #2 is slightly larger than it was in 2018. The maximum accumulation thickness is 6.54 m, which is located near the northeast corner of the residential buildings. The debris flow in the middle of gully #3 is thick and can reach approximately 5 m. The debris flow stops moving after it reaches the downstream part of the gully and never reaches the channel outlet, so it cannot affect the residents directly.

For the debris flow with a 50-year recurrence interval, in gully #1, the debris flows through the residential area at the channel outlet and arrives near the Xigou River, with the maximum accumulation thickness of approximately 6 m, so the debris flow can bury some houses in the residential area. The scope of the debris flow hazard area in gully #2 expands further and spreads to the farmland in front of the channel outlet. With an accumulation thickness of 10.18 m, the debris flow seriously threatens the lives and property of the residents in gully #2. The accumulation thickness of the debris flow in gully #3 is mostly between 6 and 9 m, and its head rushes out of the channel outlet, which gradually threatens the factory buildings.

For the debris flow with a 100-year recurrence interval, due to the proximity of the Xigou River to gully #1, the debris flows into the Xigou River, accumulates in large quantities and blocks the river, forming a barrier dam. Many debris flow in gully #2 accumulate on the farmland in front of the residential buildings, the accumulation thickness is as high as 8 m, and a small amount of debris flows into the Xigou River. The debris flow in gully #3 flows out from the channel outlet, forming a fan-shaped accumulation area with a thickness of 5 m, burying the factory buildings in front of the channel outlet.

The numerical simulation results show that in these three cases, the places near the outlet of #1, #2, and #3 gullies are the most vulnerable to debris-flow damage, while slopes and places away from the channel outlet are relatively safe. The maximum accumulation thickness of the debris flow in the 30-year recurrence interval is 6.54 m, which occurs at the outlet of gully #2 and the middle reaches of gully #3 and has a great impact on the residential buildings at the outlet of gully #2. The maximum accumulation thickness of the debris flow in the 50-year recurrence interval is 10.18 m, the accumulation thicknesses at gully #2 and the middle and lower reaches of gully #3 are high, and the buildings at each gully are greatly threatened. The debris flow in the 100-year recurrence interval has the widest influence range, the maximum accumulation thickness is 10.00 m, and the debris flow is mainly concentrated downstream of gullies #2 and #3. In this case, the buildings at the channel outlet are all impacted or even buried. The outgoing debris flow can block the river and may cause more serious disasters.

TABLE 3 Simulation parameters of the debris flow in the study area.

Basin area F (km^2)	Frequency P (%)	Bulk density γ_c (kg/m^3)	Blockage factor D_c	Sediment correction coefficient $\varnothing$	Peak flood flow Q_p(m^3/s)	Peak debris flow Q_c(m^3/s)
0.479	3.3	1.61	1.6	0.587	9.279	23.554
	2	1.61	1.7	0.587	10.034	27.063
	1	1.61	1.8	0.587	11.353	32.421

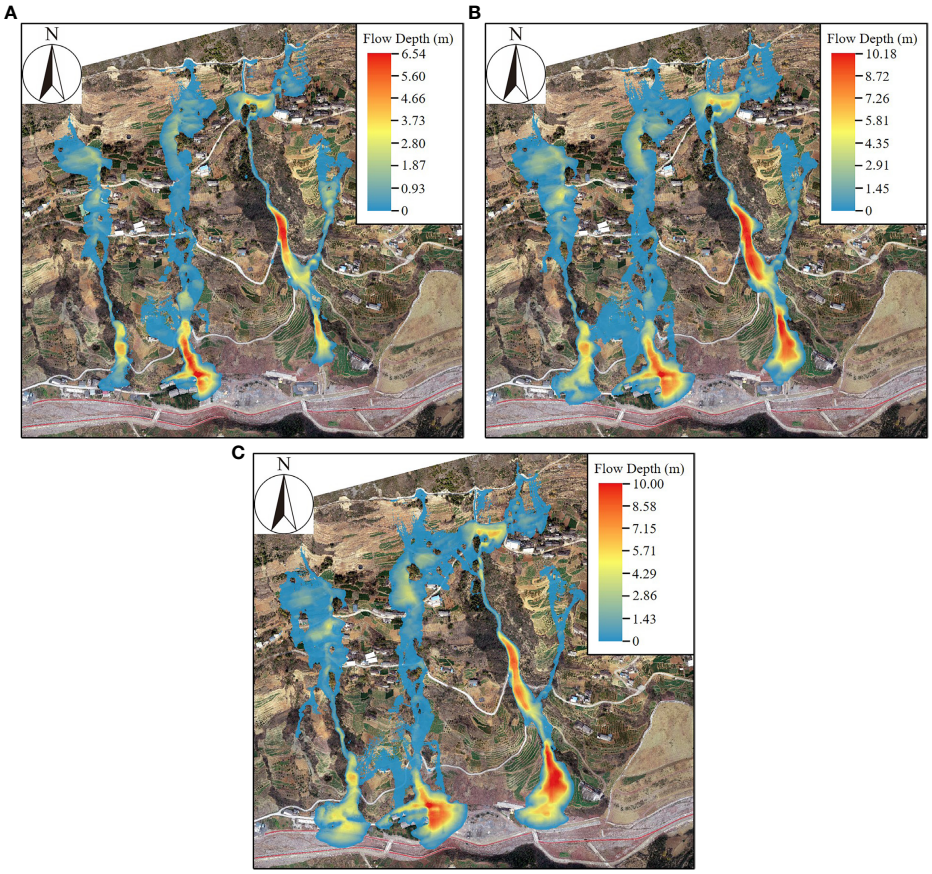

FIGURE 5
The debris flow accumulation thickness for different recurrence intervals. **(A)** 30-year recurrence interval **(B)** 50-year recurrence interval **(C)** 100-year recurrence interval.

5 Discussion

5.1 Hazard zones

In this paper, referring to Swiss and Austrian standards (Fiebiger, 1997; Garcia et al., 2004), combined with the intensity and probability of debris flow, the hazard of debris flow is divided into three levels: low, medium, and high. Debris flow intensity is defined as the combination of the maximum debris flow depth (H) multiplied by the maximum flow velocity (V) (Chang et al., 2017). The classification of debris flow intensity based on H and V is shown in Table 4. According to the classification criteria in Table 4, the classification results of debris flow intensity in different recurrence intervals are obtained (Figures 6A–C).

TABLE 4 Debris flow intensity classification.

Debris flow intensity	Maximum depth H (m)	Relation	Maximum depth (H) multiplied by maximum velocity (V) (m^2/s)
High	H>2.5	or	VH>2.5
Medium	0.5<H<2.5	and	0.5<VH<2.5
Low	0<H<0.5	and	VH<0.5

The annual probability of debris flow can be calculated by the following Equation:

$$P_m = 1 - \left(1 - \frac{1}{T}\right)^m \tag{12}$$

where P_m is the probability of debris flow occurring over m years and T is the recurrence interval of debris flow. The Taiwan Debris Flow Risk Classification (Lin et al., 2011) divides debris flows into high probability (greater than 10%), medium probability (between 10% and 1%), and low probability (between 1% and 0.2%). We specify m=1.

By combining the intensity level with the occurrence probability, the hazard of debris flow is classified, as shown in Figure 7. Based on this classification system, the map of hazard zones of the Xigou debris flow is drawn (Figure 8). The high-hazard area covers an area of 37378 m^2, accounting for 21% of the affected area, and is mainly located inside debris-flow gullies #1, #2, and #3. The medium-hazard area covers an area of 67108 m^2, accounting for 37% of the affected area, and is mainly located near gullies #1 and #2 and the landslide area. The low-hazard area covers an area of 758,559 m^2, accounting for 42% of

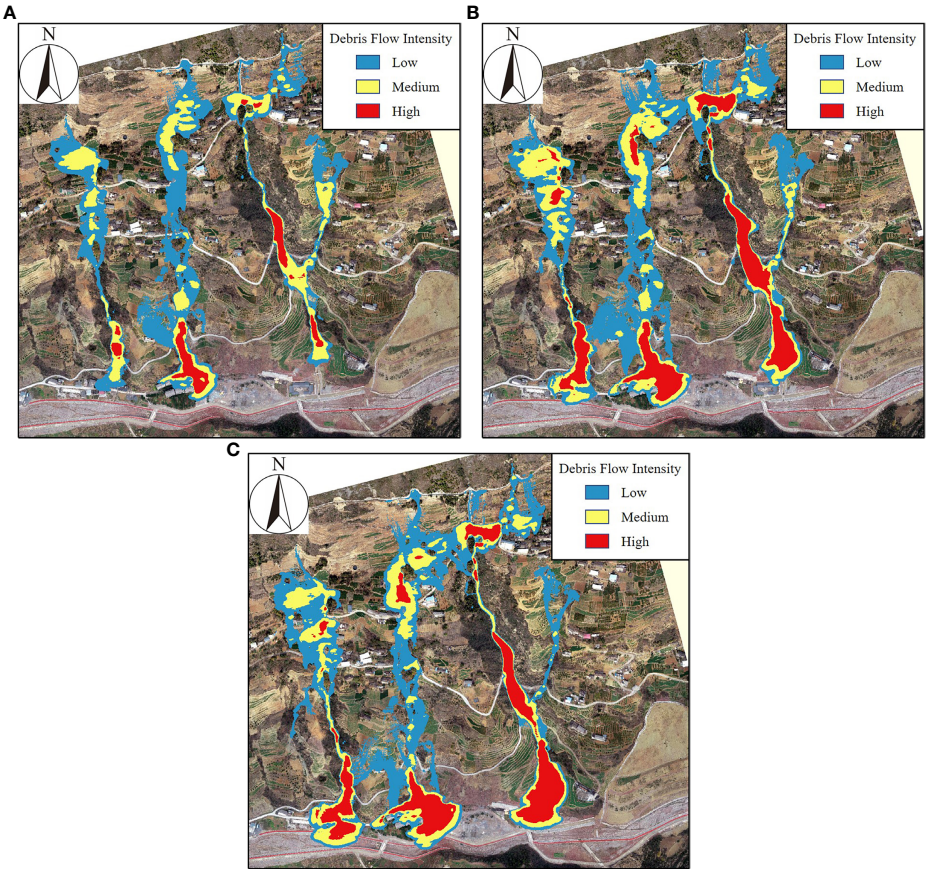

FIGURE 6
Zones of debris flow intensity for different recurrence intervals. **(A)** 30-year recurrence interval, **(B)** 50-year recurrence interval, **(C)** 100-year recurrence interval.

the affected area, and is mainly located at the upstream and channels outlet of debris flow.

5.2 Vulnerability zones

Vulnerability mainly reflects the disaster-bearing capacity of the disaster-bearing body. Cui et al. (2013) defined vulnerability according to economic loss, which is related to the economic value and degree of damage of disaster-affected objects.

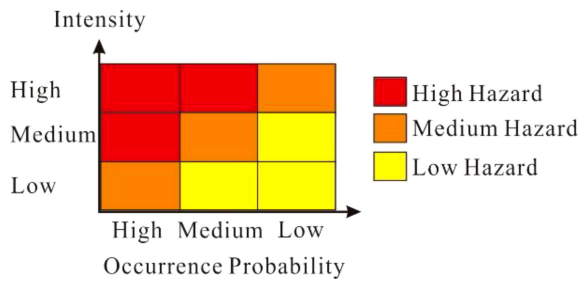

FIGURE 7
Hazard classification by debris flow intensity and occurrence probability.

$$V = V(u) \times C \tag{13}$$

where V is the degree of vulnerability; $V(u)$ is an economic index with a value range of 0 to 1; and C is an index to measure the degree of damage to disaster-affected objects, with a range of 0 to 1. $V(u)$ is the unit price $P(/m^2)$ of the disaster-affected object multiplied by its area $N(m^2)$:

$$V(u) = P \times N \tag{14}$$

According to the difference in function and value, the disaster-bearing objects of the Xigou debris flow are divided into three categories: houses, farmland (including open space), and rivers. The area N and the number of disaster-affected objects are determined according to field surveys and UAV images, and the unit price P of each disaster-affected object is determined according to the reference price provided by the government of Chongqing. C represents the degree of damage to the disaster-affected object by the impact of debris flow, and its value ranges from 0 to 1: The larger the C is, the more vulnerable the disaster-affected object is. The C of disaster-affected objects of different structural types is different. Cui et al. (2013) conducted a detailed investigation of debris flow disasters in the central and western regions of China and proposed a vulnerability index standard for different buildings or structures (Table 5). The value of C refers to Table 5. A C value of 1

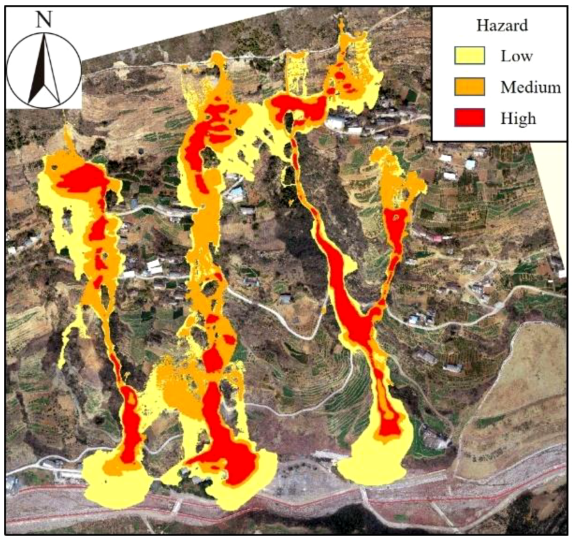

FIGURE 8
Hazard zones of the Xigou debris flow.

for agricultural land means that it can be completely damaged by a debris flow.

Finally, the vulnerability based on economic loss is calculated by Equation (14). The economic value of the vulnerability of each disaster-bearing body is superimposed on ArcGIS to obtain a map of vulnerability zones (Figure 9). Figure 9 shows that the high-vulnerability area covers an area of 9416 m^2, accounting for 6% of the affected area, and its disaster-affected objects are mainly residential buildings. The medium-vulnerability area covers an area of 3945 m^2, accounting for 3% of the affected area, and its disaster-affected objects are mainly the Xigou River. The low-vulnerability area covers an area of 140,850 m^2, accounting for 91% of the affected area, and its disaster-affected objects are mainly farmland.

5.3 Debris-flow risk zones

We adopt the expression of the risk of natural disasters such as debris flows proposed by the United Nations Department of Humanitarian Affairs in 1992:

$$R = H \times V \tag{16}$$

where R is the risk level, H is the hazard level, and V is the vulnerability level.

The map of risk zones of Xigou debris flows are obtained by a raster operation on the hazard and vulnerability results of debris flows on the ArcGIS platform (Figure 10). As shown in Figure 10, the areas affected by debris flows are divided into three risk levels: low, medium, and high. Table 6 summarizes the areas and proportions for different hazard, vulnerability, and risk levels. Among them, the high-risk area is the smallest, accounting for 2% of the total risk area, and mainly includes some houses and buildings near the #1 and #2 gullies. This area has the highest risk of debris flow in the future, and the protection of this area should be strengthened. The medium risk area covers an area of 40,531 m^2, and is mainly located inside the #1, #2, #3 debris-flow gullies. The low-risk area is the largest, accounting for 75% of the total risk area (136,025 m^2), and mainly covers large tracts of farmland and some river channels where the debris flows through. Figure 10 can provide a reference for debris flow prevention and control in the future.

6 Conclusion

In this paper, taking the debris flow in Xigou, Chongqing, China, as the research object, the RAMMS numerical simulation software and ArcGIS software are both used to simulate and analyze the 2018 debris flow event and carry out the risk assessment of debris flows with different recurrence interval when debris flows simultaneously break out in multiple gullies. We draw the following conclusions.

(1) Using RAMMS software, the Voellmy–Salm rheological model and the RKE model are used to simulate the 2018 debris flow event, whose movement and influence range are analyzed. The simulation shows that the debris flows for 400 s and the maximum accumulation thickness is 5.74 m, which happens near the northeast corner of the residential buildings.

TABLE 5 Vulnerability index of buildings or structures.

Types of structures	Vulnerability grades	Vulnerability values	Characteristics
Adobe construction	V	0.9-1.0	Small-scale debris flows can entirely destroy this type of structure.
Timber structure	IV	0.8-0.9	Small-scale or medium-scale debris flows can seriously damage this type of structure.
Brick-wood structure	III	0.5-0.8	Small-scale or medium-scale debris flows can partially destroy this type of structure.
Brick-concrete structure	II	0.2-0.5	Small-scale or medium-scale debris flows do not generally affect this type of structure, but it can be partially destroyed by large-scale debris flow.
Steel reinforced concrete structure	I	0.1-0.2	This type of structure is not generally affected in small-scale or medium-scale debris flows, but it can be partially destroyed by a devastating debris flow of huge magnitude.

*The Specification of Geological Investigation for Debris Flow Stabilization (DZ/T 0220-2006) grades debris-flow magnitude on the basis of the total runoff: the total runoff of a small-scale debris flow is less than 1×10^4 m^3, that of a medium-scale debris flow is between 1×10^4 m^3 and 10×10^4 m^3, that of a large-scale debris flow is between 10×10^4 m^3 and 100×10^4 m^3, and that of a mega debris flow is over 100×10^4 m^3.

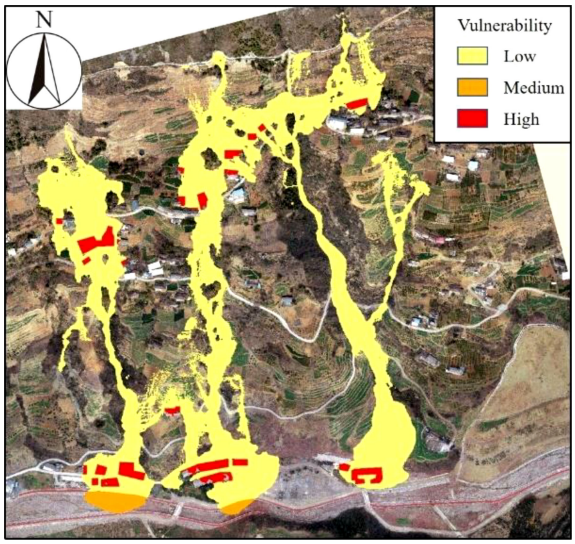

FIGURE 9
Vulnerability zones based on economic loss.

(2) The verified models and parameters are used to simulate and predict the debris flow in gullies #1, #2, and #3 in the study area and determine the potential hazard areas of debris flow in different recurrence intervals. The area around the channel outlet is most vulnerable to the hazards of debris flow, while places on the slope and away from the channel outlet are relatively safe. The maximum accumulation thicknesses of debris flow in the 30-year, 50-year, and 100-year recurrence intervals are 6.54 m, 10.18 m, and 10.00 m, respectively. The 100-year recurrence interval has the greatest influence and hazard.

(3) In this paper, referring to the disaster classification standards of Switzerland and Austria, combined with the intensity and occurrence probability of debris flow, a classification model of debris flow hazard zones with low, medium, and high-risk levels is established, and a map of hazard zones is drawn based on this classification system. From field surveys and UAV images, an economic vulnerability analysis of the disaster-bearing bodies in the study area is carried out, and a map of vulnerability zones is drawn. Finally, the hazard and vulnerability results are rasterized on the ArcGIS platform to generate a map of risk zones. The low-risk area is relatively large, accounting for 75% of the impact area of the debris flow,

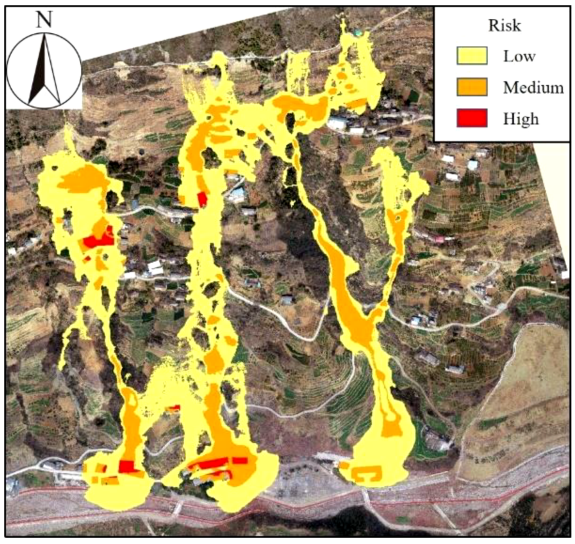

FIGURE 10
Risk zones for the Xigou debris flow.

TABLE 6 Summary of hazard, vulnerability and risk zones.

	Low	Medium	High	Total area
Hazard	75,859 m^2 (42%)	67,108 m^2 (37%)	37,378 m^2 (21%)	180,345 m^2
Vulnerability	164,114 m^2 (91%)	5410 m^2 (3%)	10,821 m^2 (6%)	
Risk	136,025 m^2 (75%)	40531 m^2 (23%)	3789 m^2 (2%)	

while the medium-risk area and high-risk area only account for 23% and 2%, respectively. The high-risk disaster-bearing bodies are mainly the buildings near the #1 and #2 gullies. The middle- and low-risk areas mainly include debris-flow gullies and nearby farmland. The high-risk area has the highest risk of damage in the event of future debris flows, so the protection of this area should be strengthened.

Data availability statement

The original contributions presented in the study are included in the article/supplementary material. Further inquiries can be directed to the corresponding author.

Author contributions

ZD: Project administration, Supervision, Writing – review & editing. AZ: Writing – original draft. WQ: Conceptualization, Writing – review and editing. XF: Formal Analysis, Writing – review and editing. JG: Software, Writing – review and editing. LG: Supervision, Writing – review and editing. LL: Visualization, Writing – review and editing. XJ: Data curation, Writing – review and editing. HW: Investigation, Writing – review and editing, Investigation, Writing – review and editing.

Funding

This study was supported by the follow-up of the Geological Disaster Prevention and Control Project in the Three Gorges area (000121 2023C C60 001 and 000121 2021C C60 001), Qianlong Plan Top Talent Project of Wuhan Center of China Geological Survey (QL2022-06).

Conflict of interest

Author WQ was employed by River Basin Hub Operation Management Center, China Three Gorges Corporation.

The remaining authors declare that the research was conducted in the absence of any commercial or financial relationships that could be construed as a potential conflict of interest.

Publisher's note

References

Calvo, B., and Savi, F. (2009). A real-world application of Monte Carlo procedure for debris flow risk assessment. *Comput. Geosciences.* 35, 967–977. doi: 10.1016/j.cageo.2008.04.002

Chang, M., Tang, C., Van Asch, T. W. J., and Cai, F. (2017). Hazard assessment of debris flows in the Wenchuan earthquake-stricken area, South West China. *Landslides* 14 (5), 1783–1792. doi: 10.1007/s10346-017-0824-9

Christen, M., Kowalski, J., and Bartelt, P. (2010). RAMMS: Numerical simulation of dense snow avalanches in three-dimensional terrain. *Cold Regions Sci. Technology.* 63 (1-2), 1–14. doi: 10.1016/j.coldregions.2010.04.005

Cui, P., Zou, Q., Xiang, L. Z., and Zeng, C. (2013). Risk assessment of simultaneous debris flows in mountain townships. *Prog. Phys. Geography.* 37 (4), 516–542. doi: 10.1177/0309133313491445

Dai, Z. W., Wang, L. Q., Fu, X. L., Huang, B. L., Zhang, S. L., Gao, X. C., et al. (2023a). Degradation of typical reverse sand-mudstone interbedded bank slope based on multi-source field experiments. *Int. J. Environ. Res. Public Health.* 20 (3), 2591. doi: 10.3390/ijerph20032591

Dai, Z. W., Yang, L., Zhang, N., Zhang, C. Y., Zhang, Z. H., and Wang, H. (2023b). Deformation characteristics and reactivation mechanism of an old landslide induced by combined action of excavation and heavy rainfall. *Front. Earth Sci.* doi: 10.3389/feart.2022.1009855

Dai, Z. W., Zhang, A. L., Wang, S. F., Fu, X. L., Yang, L. W., Jang, X. N., et al. (2023c). The development characteristics and mechanisms of the Xigou debris flow in the Three Gorges Reservoir Region. *Front. Earth Sci.* doi: 10.3389/feart.2023.1122562

Fiebiger, G. (1997). Hazard mapping in Austria. *J. Torrent Avalanche Landslide Rockfall Engineering.* 134 (61), 93–104.

Garcia, R., Rodriguez, J. J., and Brien, J. S. (2004). Hazard zone delineation for urbanized alluvial fans. *2004 ASCE World Water & Environmental Resources Congress — Arid Lands Symposium*, Salt Lake City, Utah, 2004. doi: 10.1061/40737(2004)11

Gentile, F., Bisantino, T., and Liuzzi, G. T. (2008). Debris flow risk analysis in South Gargano watersheds (Southern-Italy). *Natural Hazards.* 44, 1–17. doi: 10.1007/s11069-007-9139-9

Guo, J., Zhang, P., Zhang, Q., Huang, B. L., and Qin, Z. (2020). Study on landslide hazard identification tech-nology based on multispectral remote sensing images in wu gorge. *Geology Mineral Resour. South China* 36 (2), 38–45. doi: 10.3969/j.issn.1007-3701.2020.01.005

Lai, B., Liu, J., and Wu, S. T. (2021). Division of geological hazard inspection units based on arcGIS–– A case study of zhuhai city. *South China Geology* 37 (1), 75–82. doi: 10.3969/j.issn.2097-0013.2021.01.006

Liu, G. X., Dai, E. F., Wu, S. H., and Wu, W. X. (2012). A Study on theory and method in debris flow risk assessment. *Prog. Geography.* 31 (3), 383–391. doi: 10.11820/dlkxjz.2012.03.015

Ouyang, C. J., Wang, Z. W., An, H. C., Liu, X. R., and Wang, D. P. (2019). An example of a hazard and risk assessment for debris flows-A case study of Niwan Gully, Wudu, China. *Eng. Geology.* 263, 105351. doi: 10.1016/j.enggeo.2019.105351

Pei, Y. Q., Qiu, H. J., Yang, D. D., Liu, Z. J., Ma, S. Y., Li, J. Y., et al. (2023). Increasing landslide activity in the Taxkorgan River Basin (eastern Pamirs Plateau, China) driven by climate change. *Catena* 223, 106911. doi: 10.1016/J.CATENA.2023.106911

Qin, P. P., Huang, B. L., Li, B., Chen, X. T., and Jiang, X. N. (2022). Hazard analysis of landslide blocking a river in Guang'an Village, Wuxi County, Chongqing, China. *Landslides* 19 (11), 2775–2790. doi: 10.1007/s10346-022-01943-2

Qiu, H. J., Zhu, Y. R., Zhou, W. Q., Sun, H. S., He, J. Y., and Liu, Z. J. (2022). Influence of DEM resolution on landslide simulation performance based on the Scoops3D model. *Geomatics Natural Hazards Risk* 13 (1), 1663–1681. doi: 10.1080/19475705.2022.2097451

Tang, C., van Asch, T. W. J., Chang, M., Chen, G. Q., Zhao, X. H., and Huang, X. C. (2012). Catastrophic debris flows on 13 August 2010 in the Qingping area, southwestern China: The combined effects of a strong earthquake and subsequent rainstorms. *Geomorphology.* 139, 559–576. doi: 10.1016/j.geomorph.2011.12.021

Wang, J., Huang, B. L., Zhao, Y. B., Zhang, Z. H., and Hu, M. J. (2018). Study on deformation and failure mechanism of Huangnanbeixi dangerous rock in Three Gorges Reservoir Area. *Geology Mineral Resour. South China* 34 (4), 339–346. doi: 10.3969/j.issn.1007-3701.2018.04.009

Wang, L. Y., Qiu, H. J., Zhou, W. Q., Zhu, Y. R., Liu, Z. J., Ma, S. Y., et al. (2022). The post-failure spatiotemporal deformation of certain translational landslides may follow the pre-failure pattern. *Remote Sensing.* 14, 2333. doi: 10.3390/rs14102333

Yin, Y. P., Huang, B. L., Zhang, Q., Yan, G. Q., and Dai, Z. W. (2020). Research on recently occurred reservoir-induced Kamenziwan rockslide in Three Gorges Reservoir, China. *Landslides* 17 (8), 1–15. doi: 10.1007/s10346-020-01394-7

Yu, B., Yang, Y. H., Su, Y. C., Huang, W. J., and Wang, G. F. (2010). Research on the giant debris flow hazards in Zhouqu county, Gansu province on August 7, 2010. *J. Eng. Geology.* 18 (4), 437–444. doi: 10.3724/SP.J.1011.2010.01138

Zhang, Q., Huang, B. L., Chen, X. T., and Wang, J. (2019). Research on deformation mechanism transformation of jurassic consequent bank slope based on thickness variation of deposition layer. *Geology Mineral Resour. South China* 35 (3), 354–360. doi: 10.3969/j.issn.1007-3701.2019.03.009

Zhang, P., Ma, J. Z., Shu, H. P., and Wang, G. (2014). Numerical simulation of erosion and deposition debris flow based on FLO-2D model. *J. Lanzhou Univ. (Natural Sciences)* 50 (3), 363–368 + 375. doi: 10.1039/f19787400211

Zhang, C. Y., Yin, Y. P., Yan, H., Li, H. X., Dai, Z. W., and Zhang, N. (2021). Reactivation characteristics and hydrological inducing factors of a massive ancient landslide in the three Gorges Reservoir, China. *Eng. Geol.* 292, 106273. doi: 10.1016/j.enggeo.2021.106273

Zhang, A. L., Zhang, P., Dai, Z. W., Huang, B. L., Zhang, C. Y., Wang, L. Q., et al. (2022). Failure mechanism of the Simiqiao landslide under rainfall and slope cutting. *Arabian J. Geosciences* 15, 1432. doi: 10.1007/s12517-022-10698-y

Zou, Z. X., Luo, T., Zhang, S., Duan, H. J., Li, S. W., Wang, J. E., et al. (2023). A novel method to evaluate the time-dependent stability of reservoir landslides: exemplified by Outang landslide in the Three Gorges Reservoir. *Landslides* 20, 1731–1746. doi: 10.1007/S10346-023-02056-0

Zou, Z. X., Yan, J. B., Tang, H. M., Wang, S., Xiong, C. R., and Hu, X. L. (2020). A shear constitutive model for describing the full process of the deformation and failure of slip zone soil. *Eng. Geology* 276, 105766. doi: 10.1016/j.enggeo.2020.105766